

# Elucidating the Role of Dose in the Biopharmaceutics Classification of Drugs: The Concepts of Critical Dose, Effective *In Vivo* Solubility, and Dose-Dependent BCS

Georgia Charkoftaki · Aristides Dokoumetzidis · Georgia Valsami · Panos Macheras

Received: 21 March 2012 / Accepted: 20 June 2012  
© Springer Science+Business Media, LLC 2012

## ABSTRACT

**Purpose** To develop a dose dependent version of BCS and identify a critical dose after which the amount absorbed is independent from the dose.

**Methods** We utilized a mathematical model of drug absorption in order to produce simulations of the fraction of dose absorbed ( $F$ ) and the amount absorbed as function of the dose for the various classes of BCS and the marginal cases in between classes.

**Results** Simulations based on the mathematical model of  $F$  versus dose produced patterns of a constant  $F$  throughout a wide range of doses for drugs of Classes I, II and III, justifying biowaiver claim. For Classes I and III the pattern of a constant  $F$  stops at a critical dose  $Dose_{cr}$  after which the amount of drug absorbed, is independent from the dose. For doses higher than  $Dose_{cr}$ , Class I drugs become Class II and Class III drugs become Class IV.  $Dose_{cr}$  was used to define an *in vivo* effective solubility as  $S_{eff}=Dose_{cr}/250$  ml. Literature data were used to support our simulation results.

**Conclusions** A new biopharmaceutic classification of drugs is proposed, based on  $F$ , separating drugs into three regions, taking into account the dose, and  $Dose_{cr}$ , while the regions for claiming biowaiver are clearly defined.

**KEY WORDS** BCS · critical dose · DDBCS · dose · effective *in vivo* solubility

## INTRODUCTION

As oral administration is the most commonly used drug-dosing route, the ability to correlate the drug characteristics, such as dose, lipophilicity, aqueous solubility and permeability, with the rate and extent of absorption has been a crucial problem for many years. Such knowledge would allow scientists to select the best drug candidates early in the drug development cycle.

One start of this effort was made in 1985, when the absorption potential (AP) concept was developed (1). This was the only approach until then, that was taking into account the dose as one among the other principal parameters e.g. the 1-octanol-water partition coefficient ( $P$ ) and the intrinsic solubility of the drug for the estimation of the fraction of dose absorbed ( $F$ ). After the general correlation of AP with  $F$ , a quantitative version of this work revealed more features of the relation between AP and  $F$  and classified the drugs into three broad categories, according to their AP values in relation to the fraction of dose absorbed (2). In 1996 the maximum absorbable dose (MAD) concept was introduced by Johnson and Swindell and combined, in a conceptually simple way, four key factors that impact the extent of absorption: solubility, absorption rate constant, estimated gastrointestinal fluid volume and absorption time (3). In 1999 Yu modified this equation by replacing absorption rate constant and fluid volume with effective human intestinal permeability ( $P_{eff}$ ) and effective intestinal surface area to calculate maximum absorbable dose (4). MAD is defined as the maximum amount of drug that could be absorbed in the GI tract assuming that

---

**Electronic supplementary material** The online version of this article (doi:10.1007/s11095-012-0815-4) contains supplementary material, which is available to authorized users.

---

G. Charkoftaki · A. Dokoumetzidis · G. Valsami · P. Macheras (✉)  
Laboratory of Biopharmaceutics & Pharmacokinetics  
Faculty of Pharmacy  
National & Kapodistrian University of Athens  
Athens, Greece  
e-mail: macheras@pharm.uoa.gr

the drug is completely saturated for the entire length of the absorption time (3–5). In 1995, the seminal article of Biopharmaceutics Classification System (BCS) was published and the dose was used for the definition of the dose number (6). The BCS categorized drugs into four classes, based on fundamental parameters that determine oral drug absorption, solubility and permeability. Four biopharmaceutic drug classes were proposed and suggestions were made for setting standards for *in vitro* drug dissolution testing which would correlate with the *in vivo* process. A relevant FDA guideline (7) entitled “Waiver of *in vivo* bioavailability and bioequivalence studies for immediate release solid dosage forms based on a biopharmaceutics classification system” was issued in 2000. In this guidance, the solubility classification of a given drug relies on the highest dose strength in an immediate release product.

These advances attracted the interest of scientists for the BCS and the criteria used for the solubility and permeability classification in the FDA guidance (7). In this vein, the high solubility definition of the FDA guidance was criticized as too strict for acidic drugs like NSAIDs since they exhibit extensive gastrointestinal (GI) absorption (8). However, an explanation based on the dynamics of the two consecutive processes dissolution and GI wall permeation was provided (9). Moreover, the solubility/dose ratio was proposed (10) as a more meaningful parameter for biopharmaceutic classification purposes. Besides, Wu and Benet proposed (11) that a Biopharmaceutics Drug Disposition Classification System (BDDCS) may result in a classification system that yields predictability of *in vivo* disposition for all four classes. According to this classification system, if the major route of elimination for a drug is metabolism, then the drug would exhibit high permeability, while if the major route of elimination is renal and biliary excretion of unchanged drug, then that drug should be classified as low permeability. In fact, the recent guideline of the European Medicines Agency (EMA) adopted (12) the extent of drug metabolism (i.e. ≥85% metabolized) as an alternate method in defining Class I marketed drugs suitable for a waiver of *in vivo* studies of bioequivalence.

Recently, a collection of over 900 drugs was classified for BDDCS (13) while a computational procedure for predicting BDDCS class from molecular structures was described for new molecular entities (14). These two studies were not only based on information derived from molecular structure but also took into account the biological factors involved. A very interesting result of both studies is that the solubility/dose ratio is an important parameter for BDDCS classification. These advances (13,14) call for an in depth study of the role of the solubility/dose ratio in the biopharmaceutics classification of drugs. To this end, we utilized the original model used for the development of BCS (6) as modified by us (9) to examine in detail the effect of dose on the fraction of dose absorbed for each one of the four BCS drug classes.

Based on our modeling work, we developed the concepts of the critical dose and effective *in vivo* solubility; furthermore, real data were analyzed and estimates of the effective *in vivo* solubility were derived. Finally, these results led us to the development of a dose dependent version of BCS, the so called DDBCS in order to define the regions for claiming biowaiver.

## METHODS

The BCS article (6) was based on the tube model of the intestinal lumen (15). This model considers constant drug permeability along the intestines, a plug flow fluid with the suspended drug particles moving with the fluid, and dissolution in the small particle limit. The original system of differential equations for the change of the spherical drug particles  $r_p$ , and the change of the concentration of dissolved drug in the lumen,  $C_L$ , was expressed in terms of the axial intestinal distance,  $z$  (6,15). This system was modified by us (9) and it was rewritten in respect of time,  $t$ , since the independent variable axial intestinal distance,  $z$ , is proportional to time as the fluid flow rate is considered constant:

$$\frac{dr_p}{dt} = \begin{cases} -\frac{D}{\rho} \frac{M_0}{V_0 r_p} \left(\frac{1}{q} - \Phi\right) & \text{if } r_p > 0 \\ 0 & \text{if } r_p = 0 \end{cases} \quad (1)$$

$$\frac{d\Phi}{dt} = \frac{3D}{\rho V_0} \frac{r_p M_0}{r_0^3} \left(\frac{1}{q} - \Phi\right) - \frac{2P_{eff}}{R} \Phi \quad (2)$$

where  $D$  is the diffusion coefficient,  $\rho$  is the density of the solid drug,  $r_0$  is the initial radius of the drug particles,  $V_0$  is the luminal volume,  $R$  is the radius of the intestinal lumen,  $M_0$  is the dose,  $P_{eff}$  is the effective permeability of the drug  $\Phi$ , is the fraction of dose dissolved,  $q$  is the dimensionless dose/solubility ratio ( $q=M_0 / V_0 C_s$ ) and  $C_s$  denotes the solubility of the drug.

These equations can be coupled with the mass balance relationship which describes the fraction of dose absorbed  $F$  as a function of the dose  $M_0$ , and the undissolved and dissolved mass at the end of the tube  $M_{solids}$ ,  $M_{dissolved}$ , respectively:

$$F = \frac{M_0 - M_{solid} - M_{dissolved}}{M_0} \quad (3)$$

This equation can be simplified to:

$$F = 1 - \left(\frac{r_p}{r_0}\right)^3 - \Phi \quad (4)$$

The values of  $r_p$  and  $\Phi$  in Eq. 4 correspond to the time equal to the mean intestinal transit time. The system of differential Eqs. 1 and 2 was solved numerically in

Mathematica (see [Supplementary Material source code](#)) assigning typical values for the constants  $r_0$  (25  $\mu\text{m}$ ),  $D$  ( $1 \times 10^{-4}$   $\text{cm}^2/\text{min}$ ),  $\rho$  (1000  $\text{mg}/\text{mL}$ ),  $V_0$  (250  $\text{mL}$ ),  $R$  (1  $\text{cm}$ ) (13) to get estimates for  $r_p$  and  $\Phi$  at the end of the tube at time equal to the mean intestinal transit time, which was assigned to 200 min (16). These values were further used to get an estimate for  $F$  from Eq. 4.

Various values were assigned to solubility and permeability in order to simulate drugs belonging either to four biopharmaceutical classes or to border line cases. The dose  $M_0$  was ranged from 0 to 1500  $\text{mg}$  to simulate the clinical dose encountered in clinical practice.

## RESULTS AND DISCUSSION

### Simulations

Fig. 1 shows the simulation results for the fraction of dose absorbed  $F$  as a function of dose,  $M_0$ . These results demonstrate that the effect of dose on  $F$  varies according to the

solubility and permeability values of the drug. In three of the nine cases analyzed, the dose does not affect  $F$  since the high solubility and permeability values ensure complete absorption (Fig. 1b, c, and f) indicating that these drugs belong to Class I irrespective to the dose considered in the range 0–1500  $\text{mg}$ . Fig. 1i depicts a classical Class III drug which exhibits a constant value  $F=0.4$  irrespective of the dose used in the range 0–1500  $\text{mg}$ . This behavior is basically associated with the first-order character and the limiting behavior of the permeation process coupled with the high solubility (10  $\text{mg}/\text{mL}$ ) of the drug which enables the value of  $1/q$ , which is equal to  $V_0 C_s / M_0$ , to be higher than 1.7 for all doses examined. On the contrary, the value of  $F$  depends on dose for doses higher than 250  $\text{mg}$  when a less soluble drug is considered (Fig. 1h). This means that the drug in Fig. 1h is a classical Class III drug for doses  $\leq 250$   $\text{mg}$  while it behaves like a Class IV drug (low solubility, low permeability) for doses higher than 250  $\text{mg}$ . A typical Class IV drug is shown in Fig. 1g whereas no linear segment is observed for the whole range of doses utilized, while the limited absorption results from the lowest values assigned to solubility and

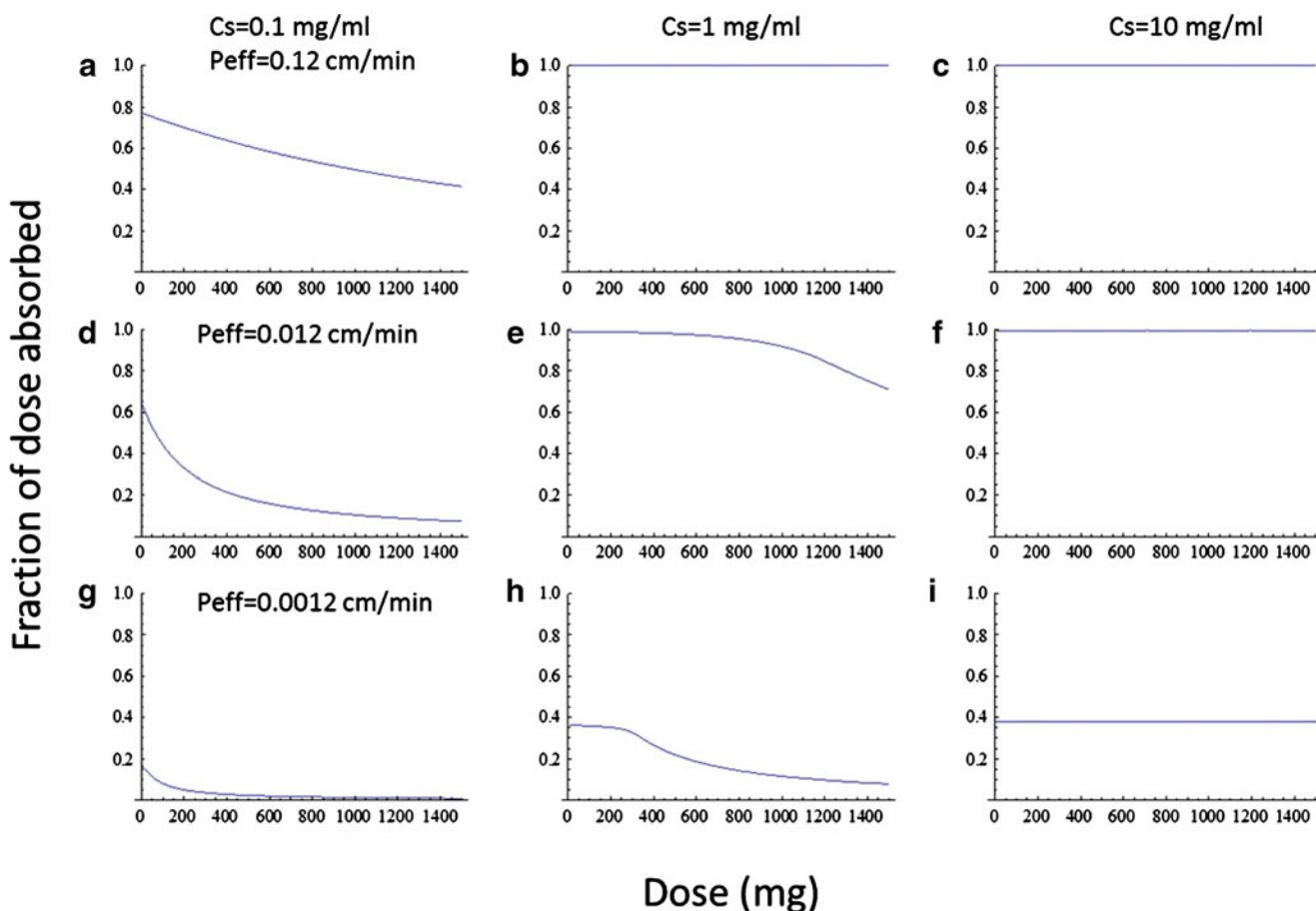


**Fig. 1** Simulation results for the fraction of dose absorbed  $F$  at time 200 mins, as a function of dose,  $M_0$ , using the Eqs. 1, 2 and 4. Parameters take the following values:  $r_0=25$   $\mu\text{m}$ ,  $D=1 \times 10^{-4}$   $\text{cm}^2/\text{min}$ ,  $\rho=1000$   $\text{mg}/\text{mL}$ ,  $V_0=250$   $\text{mL}$ ,  $R=1$   $\text{cm}$ . (**a, b, c**)  $P_{\text{eff}}=0.12$   $\text{cm}/\text{min}$ , (**d, e, f**)  $P_{\text{eff}}=0.012$   $\text{cm}/\text{min}$ , (**g, h, i**)  $P_{\text{eff}}=0.0012$   $\text{cm}/\text{min}$ . (**a, d, g**)  $C_s=0.1$   $\text{mg}/\text{mL}$ , (**b, e, h**)  $C_s=1$   $\text{mg}/\text{mL}$ , (**c, f, i**)  $C_s=10$   $\text{mg}/\text{mL}$ .

permeability. Fig. 1e illustrates a Class I drug ( $F > 0.90$ ) for doses lower than 1000 mg which exhibits a Class II drug behavior when the dose becomes higher than 1000 mg. The  $F$  versus  $M_0$  plot in Fig. 1a demonstrates a continuously decreasing pattern with respect to the dose. This is indicative of a Class II drug, the extent of absorption of which decreases with dose. Fig. 1d shows a similar dependency of  $F$  on  $M_0$  to this observed in Fig. 1a; here, however, the dependence on the dose is steeper, since the effective permeability is smaller.

Overall, linear  $F$  versus  $M_0$  plots are observed for either Class I drugs ( $F=1$ ) or for drugs with typical Class III behavior ( $F < 1$ ) for the whole range of doses studied. In both cases, a segment decreasing with dose will appear in the  $F$  versus  $M_0$  plot, for dose levels above or well above the saturation capacity of the GI fluids (e.g. 250 mL), when drug permeability is low or high, respectively. For this dose region, Class I drugs behave like Class II drugs ( $F < 0.90$ ) while Class III drugs behave like Class IV drugs. Class II and Class IV drugs present various degrees of nonlinearity in the  $F$  versus  $M_0$  plots, while in all cases  $F$  is below 0.90 for the entire dose range studied.

Although the results presented in Fig. 1 elucidate the effect of the dose on the fraction absorbed and allow conclusions to be derived in regard to the biopharmaceutical classification of drugs, a more practically useful presentation is the amount absorbed versus  $M_0$  plots, Fig. 2. In actual practice, one can use an exposure metric like the area under the curve (AUC), which is proportional to the amount absorbed, for the analysis of experimental data assuming no first-pass effect and linear uptake and disposition processes.

Furthermore, the results presented in Fig. 2 are also useful for the elucidation of important issues associated with the biopharmaceutical classification of drugs. For example, Fig. 2i demonstrates that the limited absorption of a classical Class III drug is solely dependent on its effective permeability value. Benet and co-workers (17,18) have demonstrated that effective permeability ( $P_{eff}$ ) values cannot be predictive for the extent of absorption since a permeation rate parameter (effective permeability has cm/min units) cannot be used as a predictor of extent of absorption. Although the results in Figs. 1i and 2i indicate to the contrary, the unpredictability of the effective permeability values for the extent of absorption is associated with the limitations of the model used for the development of BCS and utilized in this work too. In fact, the use of a single effective permeability value for the uptake of drug along the GI system is not in accord with the varying i) composition e.g. pH of the GI lumen fluids and ii) ionization of drug across the GI lumen fluids. Moreover, a valid estimation of  $P_{eff}$  presupposes ideal experimental conditions in line with the assumptions of the Fick's law of diffusion, which are not fulfilled under real *in vivo*

conditions due to the complexity in composition, structure and function of the GI system (19,20). More refined absorption models (21–23) take into account the heterogeneity of the GI system.

### Critical Dose and Effective *In Vivo* Solubility

The simulation results of Fig. 2 are in line with the corresponding results of Fig. 1. However, the most noteworthy feature of the simulation findings (Figs. 1 and 2) is the transition of a drug from Class I to Class II (Figs. 1e and 2e) and from Class III to Class IV (Figs. 1h and 2h). In the first case (Figs. 1e and 2e), the bend of the slope corresponds to the maximum cumulative amount absorbed since drug's permeability is high, while in the latter case (Figs. 1h and 2h), the bend of the slope is equal or slightly higher than the amount needed to saturate the GI fluids, since permeability is very low. In both cases, the transition of drug's classification from I to II or from III to IV is associated with an abrupt change of the amount absorbed versus  $M_0$  plot at a specific critical dosage,  $Dose_{cr}$  as depicted in Fig. 3 using AUC as the dependent variable.

Obviously, the  $Dose_{cr}$  is conceptually identical in both drug transition classifications (from I to II or from III to IV) indicating the minimum dose that corresponds to the highest amount of drug absorbed in a dose escalation study. However, the numerical values are different since they refer to different drugs with different biopharmaceutical properties. In principle, the lower doses than  $Dose_{crI-II}$  in the transition from Class I to Class II can get a biowaiver status if constant ratios of AUC/Dose are observed in the ascending linear segment of the graph in Fig. 3. Nevertheless, the biowaiver status of lower doses than  $Dose_{crIII-IV}$  for Class III drugs should not be applied to higher doses corresponding to the horizontal segment of Fig. 3.

Plausibly, the value of  $Dose_{cr}$  can be combined with the volume of gastrointestinal fluids, e.g. 250 mL to get a global noninvasive estimate for the effective *in vivo* solubility  $S_{eff}$  in the GI lumen:

$$S_{eff} = \frac{Dose_{cr}}{250} \quad (5)$$

Thus,  $S_{eff}$  translates the critical dose to an upper bound of a hypothetical solubility value for homogenous drug solution of 250 ml in the GI tract.

As the ability to predict whether a certain formulation has the potential of suitable drug absorption for large preclinical *in vivo* doses is crucial, there is an increasing interest for more sophisticated *in silico* techniques. In the recent work of Wuelfing *et al.* (2012), the relatively simple maximum absorbable dose (MAD) model was utilized giving important results, but only for predicting the necessary solubility for drug absorption for animal efficacy and toxicology studies (24). In the work of Ding *et al.*

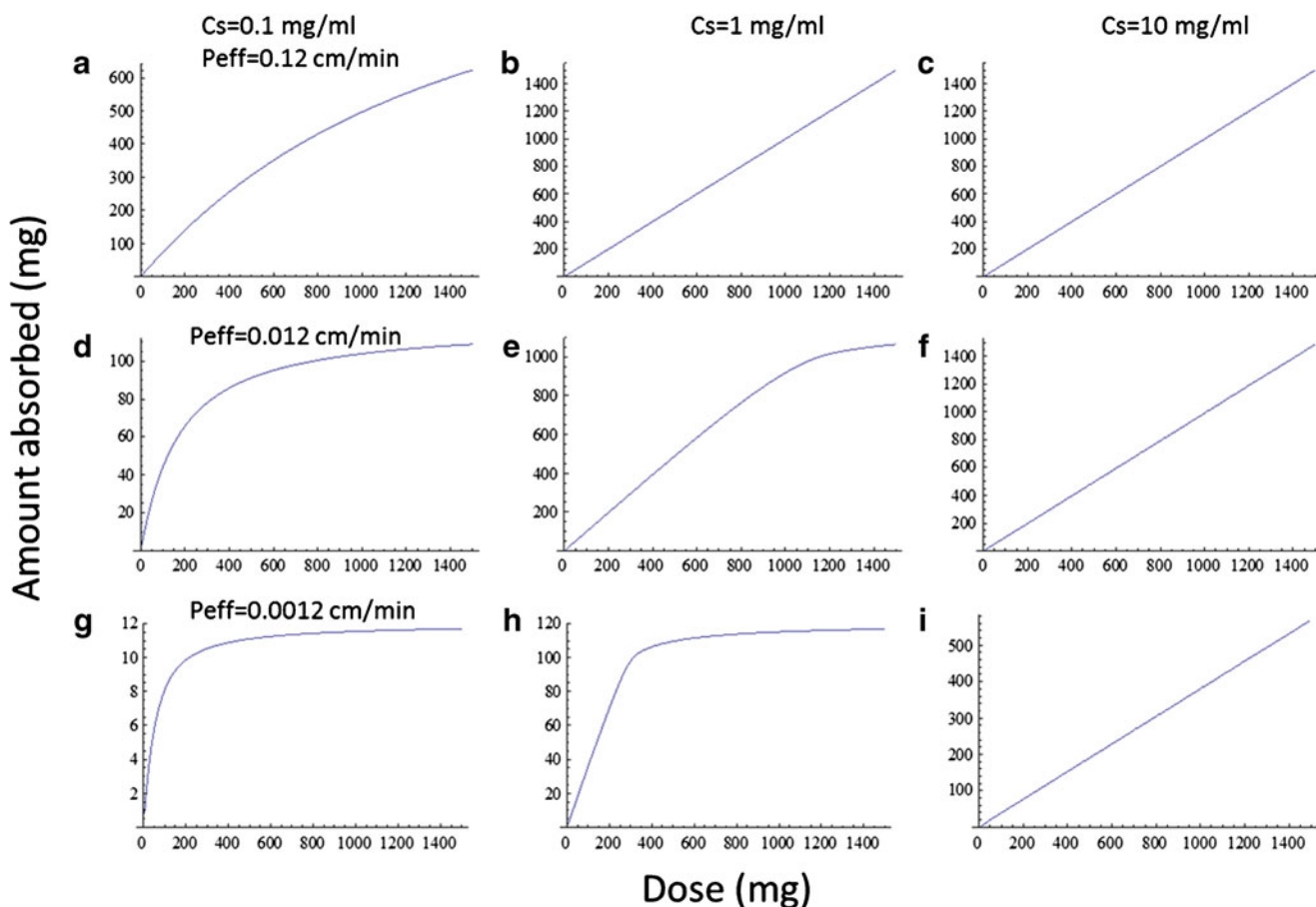


**Fig. 2** Simulation results for the amount of drug absorbed  $F \cdot M_0$ , at time 200 mins, as a function of dose,  $M_0$ , using the Eqs. 1, 2 and 4. Parameters take the same values as in Fig. 1.

(25), the authors suggested that the simplifications contained in the Yu (1999) (4) equation, provided conservative estimates of

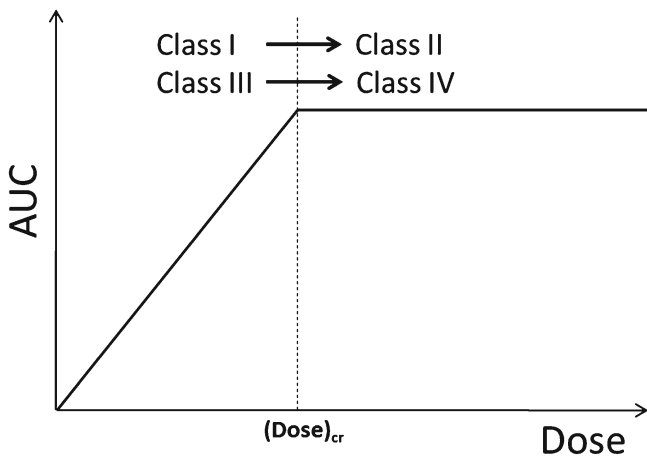


**Fig. 3** Schematic graph of AUC as a function of dose of marginal drugs, between BCS Classes I and II and classes III and IV. The extent of absorption for a drug of one of these cases exhibits two linear segments where for smaller doses the drug behaves as a class I or III, where the AUC is proportional to the dose and after a critical dose ( $Dose_{cr}$ ), different for each drug, the typical intestinal volume of 250 mL is saturated and the drug behaves as a Class II or a Class IV drug, respectively.

MAD, even with the use of computer simulation programs (e.g. Gastroplus®). It should be underlined that MAD calculation is based on a first order absorption equation and requires the knowledge of the parameters involved e.g. solubility and permeability. Our approach is based on clinical AUC *vs* dose data for the calculation of  $Dose_{cr}$ , which is combined with GI fluid volume to get an estimate for the effective *in vivo* solubility.

**Applications**

Bicalutamide has been classified as a BCS Class II drug, since is highly lipophilic, ( $\log P_{octanol/water}$  2.92) (26) while its aqueous solubility is very low (5  $\mu\text{g}/\text{mL}$ ) (26,27). According to Cockshott (27), bicalutamide obeys linear kinetics since “the  $t_{1/2}$  estimates for dosages over the whole range (10–600 mg/day) showed no apparent trend with dosage”. Analysis of steady state data reported in (28) reveals a linear relationship between the steady state concentrations,  $C_{ss}$  and dosage for the entire set of data from 10 to 200 mg (Table IV in Ref (28)); the regression line is as follows:

$$C_{ss} = 1.378 + 0.138 \times \text{Dose} \tag{6}$$

with a determination coefficient  $R^2=0.995$ . The high value of the determination coefficient for six data points based on a very large number of subjects (range 29–116) for the various doses, substantiates the linear character of the input process throughout the entire set of dosages analyzed (10–200 mg/day). Additional proof for the linearity of the input process can also be based on back extrapolation of the data with the two higher (dose,  $C_{ss}$ ) values (150 mg, 21.6 mg/L), (200 mg, 28.9 mg/L). This exercise yields the following line:

$$C_{ss} = -0.300 + 0.146 \times \text{Dose} \quad (7)$$

The slightly negative intercept of Eq. 2 using the higher dosages (150 and 200 mg), rules out the nonlinear input kinetics hypothesis since one would expect a highly positive intercept on a common sense basis. However, visual inspection of Fig. 7 in Ref (28) allows one to conclude that a patent departure from linearity in the relationship between  $C_{ss}$  and dosage is observed above 200 mg/day. In line with all above, the analysis of bicalutamide data (28) for the whole range of doses 10–600 mg using piecewise linear fitting is depicted in Fig. 4. The nice fitting of the piecewise linear function provides evidence for the proportional increase of  $C_{ss}$  as a function of dose over the dose range 10–200 mg. The intersection of the two linear segments provides an estimate for the critical dose,  $\text{Dose}_{cr}$ , for bicalutamide, equal to 230 mg. From Eq. 5 one obtains an estimate for the effective solubility,  $S_{eff}$ , of bicalutamide equal to 0.92 mg/mL. This value is 184 times higher than the aqueous solubility, 5  $\mu\text{g}/\text{mL}$ , reported in the literature (27,28) as applied to a number of studies concerning class II drugs (except for cimetidine which belongs to Class III) published in literature. The results obtained from the entire set of data analyzed, are presented in Table I and two representative plots are illustrated in Fig. 5a and b. All the data of the studied drugs were plotted ( $\text{AUC}_{0-\infty}$  versus dose) and the critical dose ( $\text{Dose}_{cr}$ ), was determined from each plot. This value

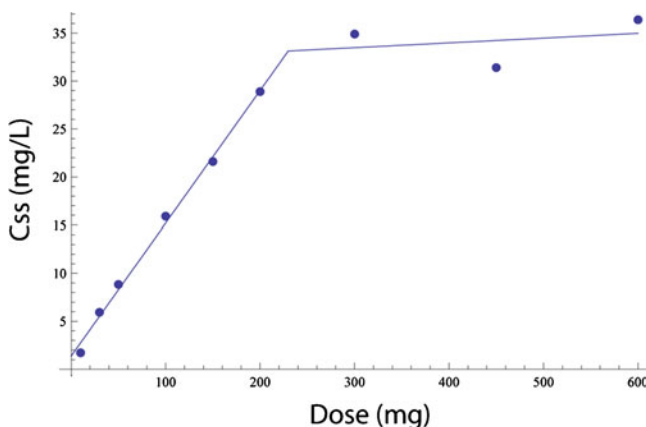


**Fig. 4** A piecewise linear fit to the entire set of bicalutamide data (dose,  $C_{ss}$ ) listed in Table IV of Ref (28). The two lines intersect at  $\text{Dose}_{cr}=230$  mg.

**Table I** Analysis of  $\text{AUC}_{0-\infty}$  Vs Dose Plots of Class II Drugs: Estimates for  $\text{Dose}_{cr}$ ,  $S_{eff}$  and Comparison with Aqueous Solubility Values

Class II Drugs	Slope ( $\pm$ SD) (h/L)	Intercept ( $\pm$ SD) ( $\text{mg} \times \text{L}^{-1} \times \text{h}$ )	$R^2$	Dose range (mg)	$\text{Dose}_{cr}$ (mg)	$S_{eff}$ (mg/mL)	Aqueous Solubility, $S_{aq}$ mg/mL (conditions)	Ratio $S_{eff}/S_{aq}$	References
Bicalutamide	0.138 (0.004)	1.378 (0.521)	0.9955	10–600	230	0.92	$5 \times 10^{-3}$	184	(27,28)
Didofenac	0.0359 (0.0003)	-0.16 (0.02)	0.9883	12.5–150	100	0.4	$6.06 \times 10^{-3}$ (25°C)	>66	(29–34)
Ibuprofen	0.171 (0.004)	7.463 (3.07)	0.9989	200–1200	1200	4.8	0.049	97.96	(50–53)
Rifampicin	0.132 (0.050)	-4.57 (23.7)	0.8657	300–600	>600	>2.4	1.5 (30°C, Form II)	>1.6	(54–58)
Atorvastatin-Ca	0.000315 ( $5.66 \times 10^{-5}$ )	2.634 (4.25)	0.9687	20–40	>40	>0.16	0.142 (27°C)	>1.13	(59–63)
Org 31710	0.64 (0.06)	-0.6 (1.0)	0.9884	10–75	25	0.1	1.74 (bile pH 6.5)	0.06	(64)
Flubiprofen	0.74 (0.01)	9.894 (2.487)	0.9994	100–300	>300	>1.2	0.008	>150.8	(65)
Fenoprofen-Ca	0.3549 (0.009)	-1.9 (2.0)	0.9992	60–300	>300	>1.2	2.8	>0.43	(66)
Ketoprofen (S enantiomer)	0.202 (0.001)	-0.2 (0.07)	0.9999	12.5–50	50	>0.2	0.01	>20	(35–37)
Prednisone	73.104 (2.89)	644.17 (119.4)	0.9953	5–80	>80	>0.12	0.223	>0.54	(67)
Cimetidine <sup>a</sup>	0.020 (0.004)	0.849 (2.09)	0.9603	100–800	>800	>3.2	5	>0.64	(68,69)

<sup>a</sup> Cimetidine is a BCS Class III drug

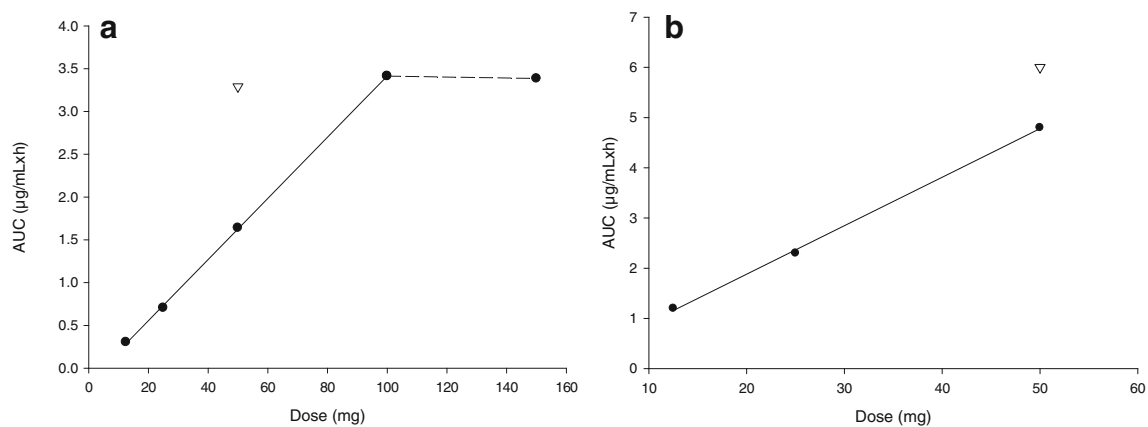


**Fig. 5** Plots of (a) diclofenac and (b) ketoprofen (S enantiomer) presenting AUC vs dose data after oral (●) and iv (▽) administration (data taken from refs (29–37)).

(Table I,  $Dose_{cr}$ ), was either the point of the intersection of the two linear segments of the plot (Fig. 5a) or a value higher than the highest dose of the  $AUC_{0-\infty}$  versus dose plot (Fig. 5b). In Table I, the effective solubility value ( $S_{eff}$ ) was calculated using Eq. 5. In all studied cases, except for fenopropfen-Ca, prednisone, Org313710 and cimetidine, this value was higher than the aqueous solubility,  $S_{aq}$  and this is demonstrated by the ratio  $S_{eff}/S_{aq}$  that was calculated (Table I). For drugs such as diclofenac, ibuprofen, flubiprofen and ketoprofen, this ratio ranged from >20 up to >150, which denotes a significant difference between the effective solubility and the experimentally obtained aqueous solubility. For fenopropfen-Ca, prednisone and cimetidine, the value of this ratio was low (>0.4), but this can be explained by the fact that the  $Dose_{cr}$  value was determined by the highest dose available from the  $AUC_{0-\infty}$  versus dose plot. The preferable critical dose value, which would provide the actual ratio and not the ‘higher than’ estimated one, would be the point of the intersection of the two linear segments of the  $AUC_{0-\infty}$  versus dose plot. This point was not available for the most of the data, as pharmacokinetic studies are performed only for a limited dose range. For Org313710, the ratio  $S_{eff}/S_{aq}$  was very low (Table I) but this was expected, as the solubility value available for the calculation of the ratio was in bile (pH 6.5), which is rather high (1.74 mg/mL). In Fig. 5a are presented the  $AUC_{0-\infty}$  versus dose data for diclofenac (29–34). It is obvious that there is  $AUC_{0-\infty}$ -dose proportionality for the first segment of the plot after oral administration of diclofenac (dose range from 12.5 up to 100 mg). The higher  $AUC_{0-\infty}$  value after intravenous administration than the one after oral administration of the same dose is explained by the 40–50% first pass effect of diclofenac (29). In Fig. 5b are illustrated the data for ketoprofen (35,36) which demonstrate a dose linearity. The  $AUC_{0-\infty}$  ketoprofen data that were plotted (Fig. 5b) correspond to S-enantiomer concentration which is the active drug moiety. Dose linearity is illustrated in Fig. 5b for doses from 12.5 up to 50 mg. The

difference observed between intravenous and oral  $AUC_{0-\infty}$  values (50 mg dose) can be explained by the first pass effect (about 40–50%) and the about 10% R to S inversion upon oral administration of ketoprofen (37).

It should be mentioned here that all calculations for effective solubility ( $S_{eff}$ ) were based on a constant gastrointestinal fluid volume, 250 mL. However, this quantity varies *in vivo* because of the high variability of the GI conditions; in other studies (10,38) a volume of 500 mL has been also considered. This is inherently associated with the heterogeneity and the dynamics of the processes in the GI tract (39). Besides, high solubility values have been found in studies dealing with the solubility and dissolution properties of poorly soluble drugs in food-mimicking (40–42) and biorelevant media (39,41). In addition, supersaturated solubility data are frequently reported in studies measuring drug concentrations in human aspirates (43,44). In most of these studies, the solubility data in human gastric aspirates have high intra- and inter-subject variability (44) while the solubilizing capacity of human intestinal fluids in the fed state is strongly time-dependent (45). Although the high values for the ratio  $S_{eff}/S_{aq}$  listed in Table I are in agreement with the above observations, the estimates of the effective *in vivo* solubility,  $S_{eff}$ , provide an upper bound for *in vivo* solubility. This type of analysis if applied to bioavailability data archives in drug agencies can lead to reliable  $S_{eff}$  estimates for a number of drugs. These estimates can be further used as a guide for developing dissolution media most akin to the *in vivo* conditions. Plausibly, the reliability of  $S_{eff}$  estimates is dependent on the experimental errors associated with the AUC values as well as the number of data points and the shape of the AUC versus dose plots.

### Dose-Dependent BCS (DDBCS)

From all above, the critical role of dose and solubility/dose ratio for biopharmaceutics classification of drugs becomes

obvious. Fig. 6 clearly depicts this. Using the modified tube model described by Eqs. 1–3, four contour plots were constructed for two levels of fraction absorbed, namely 0.20 and 0.90, in respect to solubility and effective permeability (given in logarithmic scale), for four drugs with different values of solubility and dose. The coordinates of the plots are the principal parameters of BCS (solubility and permeability); therefore one can relate  $F$  with the current use of BCS. Thus, one can classify drugs with fraction of dose absorbed,  $F \geq 0.90$  in Class I. Drugs with limited absorption ( $F \leq 0.20$ ) can be classified in Class IV while, drugs with  $F$  values in the range 0.20–0.90 can be plausibly characterized as Class II or III. Fig. 6 gives a global view of the solubility and permeability values associated with either 0.90 or 0.20 of fraction absorbed in contrast to the discrete classification into the four BCS classes. The almost perpendicular nature of the limbs of the two lines for highly permeable, low dosed drugs explains the well known steep almost piecewise linear dependence of  $F$  on

$P_{eff}$  presented in the BCS article (6). The plots in Fig. 6 reveal that only class I is compatible with the solubility-permeability criteria of BCS.

Due to continuous-quantitative nature of the plots the definitions in regard to solubility and permeability of classes II, III, IV in BCS are not fully compatible with their classification in terms of fraction absorbed. For example, the low region of  $F$  values  $< 0.20$  indicates that apart from class IV drugs various portions of class II and III lie within this category depending on the dose considered. It is also obvious that the boundary of  $F=0.90$  is solubility-dose dependent since the respective curve moves towards class II as the dose and solubility are increased. Overall, the theoretical line for  $F=0.90$  seems to be liberal for higher doses and becomes conservative for lower doses when contrasted to the perpendicular solubility borderline between classes I and II.

This analysis in conjunction with the simulation results presented in Figs. 1 and 2, indicate that the model based on

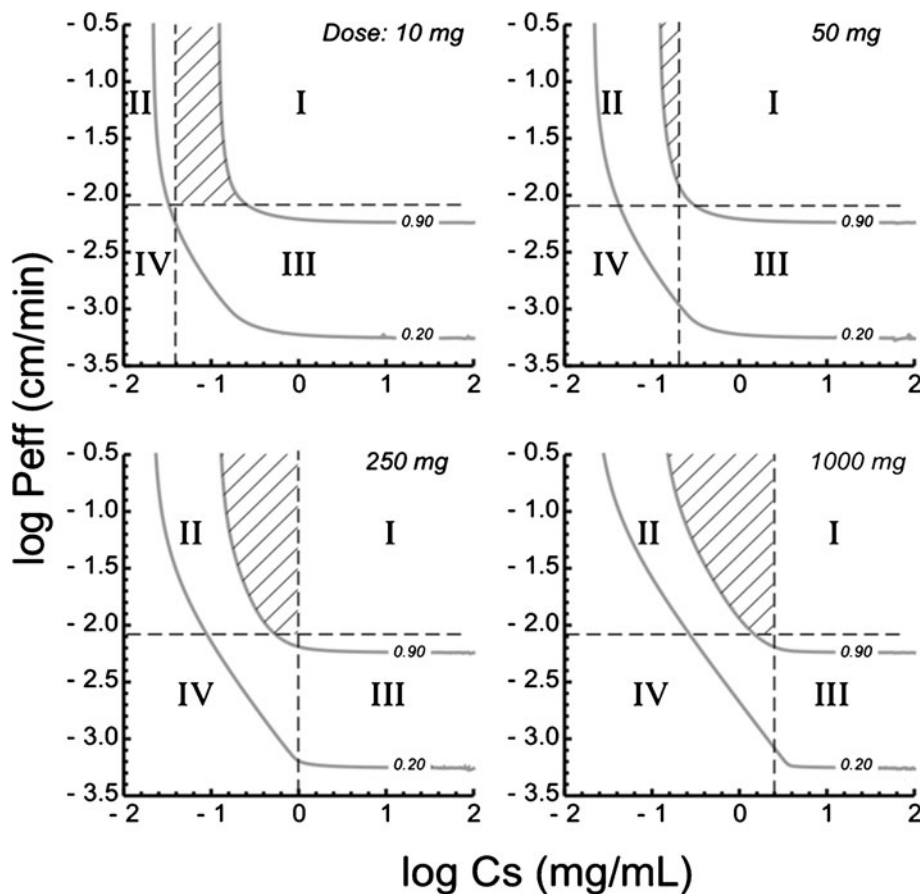


**Fig. 6** Four contour plots of two levels of fractions absorbed  $F=0.20$  and  $F=0.90$  are shown in respect to solubility ( $C_s$ ) and effective permeability  $P_{eff}$  which are denoted on logarithmic scales. The four plots correspond to four different doses 10, 50, 250 and 1000 mg, respectively and are generated by simulation using the model of Eqs. 1–4. The horizontal dashed lines on each of the plots correspond to the value  $P_{eff}=0.8 \times 10^{-2}$  cm/min, which corresponds to the permeability value of metoprolol and it is considered to be the borderline between Classes I, III and II, IV of the BCS. The perpendicular dashed lines correspond to the values of solubility where the respective dose of drug, for each of the four doses, dissolves completely in 250 ml of volume. So, it corresponds to the value given by  $C_s = \text{Dose}/(250 \text{ mL})$  for each of the four doses, namely 0.04, 0.2, 1, 4 mg/ml, respectively. These values are considered to be the borderline between Classes I, II and III, IV of the BCS. The line-shaded areas emphasise the difference of the perpendicular lines corresponding to BCS solubility borderlines, and the simulated contour lines of  $F=0.90$ . The other model parameters in the simulation are given the same as in Fig. 1.



Eqs. 1–4, leads to a dose dependent prediction of fraction absorbed and provides the basis for a dose dependent biopharmaceutics classification system (DDBCS), Fig. 7.

According to DDBCS in Fig. 7, drugs are classified based on their fraction absorbed values, depending on the administered dose, in three regions defined by the perpendicular dashed lines drawn over  $F=0.90$  and  $F=0.20$ . Drugs with  $F \geq 0.90$  are completely absorbed. Obviously, typical BCS Class I drugs belong to this region. However, BCS Class II drugs may also be classified as completely absorbed ( $F \geq 0.90$ ) depending on the administered dose. More specifically, for doses  $\leq \text{Dose}_{\text{cr I-II}}$ , BCS Class II drugs behave as Class I drugs with  $F \geq 0.90$  and biowaiver can be claimed. On the contrary, for doses  $> \text{Dose}_{\text{cr I-II}}$  these drugs are not completely absorbed and belong to the middle region ( $0.20 < F < 0.90$ ). Similarly, BCS Class I drugs may behave as BCS Class II drugs for doses  $> \text{Dose}_{\text{cr I-II}}$  and classified in the middle region of Fig. 7. BCS Class III drugs also belong to the middle region of Fig. 7 with  $0.20 < F < 0.90$  while BCS Class IV drugs are located in the region with  $F \leq 0.20$ . It should be noticed that the similarity in the interchange between BCS Class I and Class II drugs, as well as between BCS Class III and Class IV drugs relies on dose exclusively.

Using the critical dose values calculated and shown in Table I coupled with  $F$  values from literature, we classified a number of typical Class II drugs in DDBCS as shown in Fig. 7. For doses  $> \text{Dose}_{\text{cr I-II}}$  these drugs behave as typical Class II drugs, while for doses  $\leq \text{Dose}_{\text{cr I-II}}$  are completely absorbed and behave as Class I drugs. Similar experimental observations based on linear AUC-dose plots for the entire therapeutic dose range, prompted the publication of biowaiver monographs for various Class II drugs; some of these drugs are listed among the drugs of Table I (46–49).

## CONCLUSIONS

In this study we utilized a minimal mathematical model of drug absorption in order to produce simulations of the  $F$  and the amount of drug absorbed as function of the dose for the various classes of the BCS as well as the marginal cases in between classes. Our simulations based on the mathematical model of  $F$  versus dose produced patterns of a constant  $F$  throughout a wide range of doses for drugs of Classes I, II and III, justifying biowaiver claim. For Classes I and III the pattern of a constant  $F$  stops at a critical dose  $\text{Dose}_{\text{cr}}$  after which the amount of drug absorbed, is independent from the dose.  $\text{Dose}_{\text{cr}}$  was used to define an *in vivo* effective solubility,  $S_{\text{eff}}$ , which can be a helpful quantity to design *in vitro* dissolution media. Based on our simulations and the literature data shown that support these, we believe that the use of the highest dose strength for solubility classification in the BCS guideline (6) should be reconsidered and instead the dose should be used explicitly. We propose, therefore, a new biopharmaceutic classification of drugs, the DDBCS, based on  $F$ , separating drugs into three regions, taking into account the dose, and  $\text{Dose}_{\text{cr}}$ . Thus, biowaivers can be granted for lower dose strengths of certain drugs, which is not applicable for the highest dose strength. This idea is in accordance with the findings of several biowaiver monographs, proposing that biowaivers could be claimed for various Class II drugs, based on the proportionality of AUC with the dose (46–49). Further, extensive QSPR studies (13,14) about the prediction of bioavailability from molecular descriptors have found that the dose is one of the most important covariates and cannot be ignored, a fact which strengthens the idea that a biopharmaceutic classification of drugs should take into account the dose explicitly.

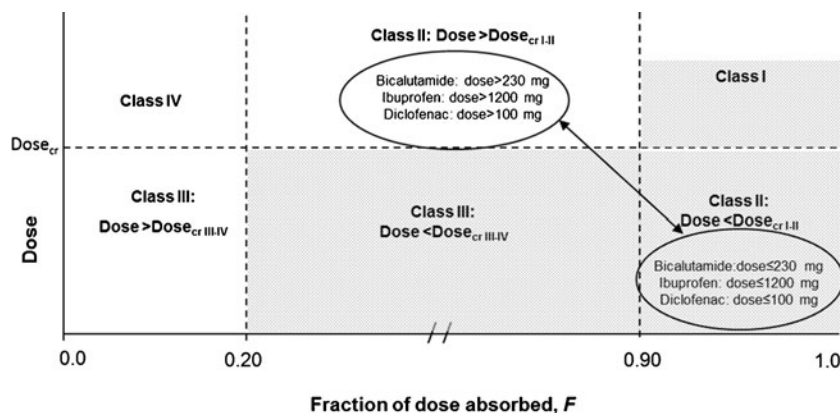


**Fig. 7** Dose Dependent Biopharmaceutic Classification System (DDBCS): Three regions are defined by the perpendicular dashed lines corresponding to 0.20 and 0.90 fraction of dose absorbed,  $F$ . These regions correspond to Class I ( $F \geq 0.90$ ), Class II & III ( $0.20 < F < 0.90$ ) and Class IV ( $F \leq 0.20$ ) of BCS, respectively. However, Class II drugs with dose  $< \text{Dose}_{\text{cr I-II}}$  behave as class I and biowaiver can be considered. Also, Class III drugs with Dose  $> \text{Dose}_{\text{cr III-IV}}$  behave as Class IV drugs. For Class III drugs with dose  $< \text{Dose}_{\text{cr III-IV}}$  absorption is only permeability dependent and a biowaiver can be also considered. The shaded area denotes biowaiver status. Classification of typical BCS Class II drugs according to the dose into either Class II or Class I of DDBCS, is also presented.

Finally, a promising future application of DDBCS could be on paediatric populations, as the range of dosage regimen is different between adults and children.

## REFERENCES

- Dressman JB, Amidon GL, Fleisher D. Absorption potential: estimating the fraction absorbed for orally administered compounds. *J Pharm Sci.* 1985;74(5):588–9.
- Macheras PE, Symillides MY. Toward a quantitative approach for the prediction of the fraction of dose absorbed using the absorption potential concept. *Biopharm Drug Dispos.* 1989;10(1):43–53.
- Johnson KC, Swindell AC. Guidance in the setting of drug particle size specifications to minimize variability in absorption. *Pharm Res.* 1996;13:1795–8.
- Yu LX. An integrated model for determining causes of poor oral drug absorption. *Pharm Res.* 1999;16:1883–7.
- Takano R, Kataoka M, Yamashita S. Integrating drug permeability with dissolution profile to develop IVIVC. *Biopharm Drug Disp.* 2012;doi:10.1002/bdd.1792.
- Amidon G, Lennernas H, Shah V, Crison J. A theoretical basis for a biopharmaceutics drug classification: the correlation of *in vitro* drug product dissolution and *in vivo* bioavailability. *Pharm Res.* 1995;12(3):413–29.
- Guidance for Industry. Waiver of *in vivo* bioavailability and bioequivalence studies for immediate release solid oral dosage forms based on a biopharmaceutics classification system. Washington, D.C.: CDER/FDA; 2000.
- Yazdani M, Briggs K, Jankovsky C, Hawi A. The "high solubility" definition of the current FDA Guidance on Biopharmaceutical Classification System may be too strict for acidic drugs. *Pharm Res.* 2004;21(2):293–9.
- Rinaki E, Dokoumetzidis A, Valsami G, Macheras P. Identification of bio waivers among Class II drugs: theoretical justification and practical examples. *Pharm Res.* 2004;21(9):1567–72.
- Rinaki E, Valsami G, Macheras P. Quantitative biopharmaceutics classification system: the central role of dose/solubility ratio. *Pharm Res.* 2003;20(12):1917–25.
- Wu CY, Benet LZ. Predicting drug disposition via application of BCS: transport/absorption/ elimination interplay and development of a biopharmaceutics drug disposition classification system. *Pharm Res.* 2005;22(1):11–23.
- EMA (European Medicines Agency). Committee for Medicinal Products for Human Use, CHMP. Guideline on the Investigation of Bioequivalence, London. 2010.
- Benet LZ, Broccatelli F, Oprea TI. BDDCS applied to over 900 drugs. *AAPS J.* 2011;13(4):519–47.
- Broccatelli F, Cruciani G, Benet LZ, Oprea TI. BDDCS Class prediction for new molecular entities. *Mol Pharm.* 2012;9(3):570–80.
- Oh DM, Curl RL, Amidon GL. Estimating the fraction dose absorbed from suspensions of poorly soluble compounds in humans: a mathematical model. *Pharm Res.* 1993;10(2):264–70.
- Yu LX, Crison JR, Amidon GL. Compartmental transit and dispersion model analysis of small intestinal transit flow in humans. *Int J Pharm.* 1996;140(1):111–8.
- Benet LZ. Predicting drug disposition via application of a Biopharmaceutics Drug Disposition Classification System. *Basic Clin Pharmacol Toxicol.* 2010;106(3):162–7.
- Benet LZ, Larregieu CA. The FDA should eliminate the ambiguities in the current BCS bio waiver guidance and make public the drugs for which BCS bio waivers have been granted. *Clin Pharmacol Ther.* 2010;88(3):405–7.
- Macheras P, Argyrakakis P. Gastrointestinal drug absorption: is it time to consider heterogeneity as well as homogeneity? *Pharm Res.* 1997;14(7):842–7.
- Dokoumetzidis A, Macheras P. IVIVC of controlled release formulations: physiological-dynamical reasons for their failure. *J Control Release.* 2008;129(2):76–8.
- GastroPlus™ Simulation Plus inc. Available from: <http://www.simulations-plus.com/Products.aspx?grpID=3&cID=16&pID=11>.
- SimCyp®, Population-based pharmacokinetic modeling and simulation. Available from: <http://www.simcyp.com>.
- PK-Sim® Available from: <http://www.systems-biology.com/products/pk-sim.html>.
- Wuelfing WP, Kwong E, Higgins J. Identification of suitable formulations for high dose oral studies in rats using *in vitro* solubility measurements, the maximum absorbable dose model, and historical data sets. *Mol Pharm.* 2012;7(9):1163–74.
- Ding X, Rose JP, Van Gelder J. Developability assessment of clinical drug products with maximum absorbable doses. *Int J Pharm.* 2012;427(2):260–9.
- Abu-Diak OA, Jones DS, Andrews GP. Understanding the performance of melt-extruded poly(ethylene oxide)-bicalutamide solid dispersions: characterisation of microstructural properties using thermal, spectroscopic and drug release methods. *J Pharm Sci.* 2012;101(1):200–13.
- Cockshott ID, Oliver SD, Young JJ, et al. The effect of food on the pharmacokinetics of the bicalutamide ("Casodex") enantiomers. *Biopharm Drug Disp.* 1997;18(6):499–507.
- Cockshott ID. Bicalutamide. *Clinical pharmacokinetics and metabolism.* *Clin Pharmacok.* 2004;43(13):855–78.
- Willis JV, Kendall MJ, Flinn RM, Thornhill DP, Welling PG. The pharmacokinetics of diclofenac sodium following intravenous and oral administration. *Eur J Clin Pharmacol.* 1979;16(6):405–10.
- Leucuța A, Vlase L, Farcau D, Nanulescu M. No effect of short term ranitidine intake on diclofenac pharmacokinetics. *Rom J Gastroenterol.* 2004;13(4):306–8.
- Hinz B, Hug AM, Fotopoulos G, Gold MS. Bioequivalence study of low-dose diclofenac potassium tablet formulations. *Int J Clin Pharmacol Ther.* 2009;47(10):643–8.
- De Bernardi di Valserra M, Feletti F, Bertè F, Nazzari M, Cenedese A, Cornelli U. Lack of effect of a single-dose of sulglycotide on the bioavailability of diclofenac. *Eur J Clin Pharmacol.* 1988;34(2):211–2.
- Biasia G, Canova N, Palazzini E, Marcolongo R. Comparative pharmacokinetic study of a single dose of two prolonged-release formulations of diclofenac in healthy subjects. *Current Ther Res.* 1998;59(1):785–92.
- Llinàs A, Burley JC, Box KJ, Glen RC, Goodman JM. Diclofenac solubility: independent determination of the intrinsic solubility of three crystal forms. *Med Chem.* 2007;50(5):979–83.
- Shohin I, Kulich J, Ramenskaya GV, Vasilenko GF. Evaluation of *in vitro* equivalence for drugs containing BCS class II compound ketoprofen. *Dissol Tech.* 2011;18:26–9.
- Geisslinger G, Menzel S, Wissel K, Brune K. Pharmacokinetics of ketoprofen enantiomers after different doses of the racemate. *Br J Clin Pharmacol.* 1995;40:73–5.
- Jamali F, Brocks DR. Clinical pharmacokinetics of ketoprofen and its enantiomers. *Clin Pharmacokinet.* 1990;19(3):197–217.
- Papadopoulou V, Valsami G, Dokoumetzidis A, Macheras P. Biopharmaceutics classification systems for new molecular entities (BCS-NMEs) and marketed drugs (BCS-MD): theoretical basis and practical examples. *Int J Pharm.* 2008;361:70–7.
- Weitschies W, Wedemeyer RS, Kosch O, Fach K, Nagel S, Söderlind E, Trahms L, Abrahamsson B, Mönnikes H. Impact of the intragastric location of extended release tablets on food interactions. *J Control Release.* 2005;108(2–3):375–85.
- Macheras P, Koupparis M, Antimisiaris S. Drug binding and solubility in milk. *Pharm Res.* 1990;7(5):537–41.

41. Galia E, Nicolaidis E, Hoerter D, Loebenberg R, Reppas C, Dressman J. Evaluation of various dissolution media for predicting *in vivo* performance of class I and II drugs. *Pharm Res*. 1998;15(5):698–705.
42. Charkoftaki G, Kytariolos J, Macheras P. Novel milk-based oral formulations: proof of concept. *Int J Pharm*. 2010;390(2):150–9.
43. Kalantzi L, Persson E, Polentarutti B, Abrahamsson B, Goumas K, Dressman J, Reppas C. Characterization of the human upper gastrointestinal contents under conditions simulating bioavailability/bioequivalence studies. *Pharm Res*. 2006;23(1):1373–81.
44. Brouwers J, Tack J, Augustijns P. *In vitro* behavior of a phosphate ester prodrug of amprenavir in human intestinal fluids and in the Caco-2 system: Illustration of intraluminal supersaturation. *Int J Pharm*. 2007;336(2):302–9.
45. Clarysse S, Psachoulas D, Brouwers J, Tack J, Annaert P, Duchateau G, Reppas C, Augustijns P. Postprandial changes in solubilizing capacity of human intestinal fluids for BCS Class II drugs. *Pharm Res*. 2009;26(6):1456–66.
46. Potthast H, Dressman JB, Junginger HE, Midha KK, Oeser H, Shah VP, Vogelpoel H, Bardens DM. Biowaiver monographs for immediate release solid oral dosage forms: ibuprofen. *J Pharm Sci*. 2005;94(10):2121–31.
47. Jantravid E, Prakongpan S, Dressman JB, Amidon GL, Junginger HE, Midha KK, Bardens DM. Biowaiver monographs for immediate release solid oral dosage forms: cimetidine. *J Pharm Sci*. 2006;95(5):974–84.
48. Chuasuwan B, Binjedoh V, Polli JE, Zhang H, Amidon GL, Junginger HE, Shah MKK, *et al*. Biowaiver monographs for immediate release solid oral dosage forms: diclofenac sodium and diclofenac potassium. *J Pharm Sci*. 2009;98(4):1206–19.
49. Becker C, Dressman JB, Junginger HE, Kopp S, Midha KK, Shah VP, Stavchansky S, Bardens DM. Biowaiver monographs for immediate release solid oral dosage forms: rifampicin. *J Pharm Sci*. 2009;98(7):2252–67.
50. Bookstaver BP, Miller AD, Rudisill CN, Norris B. Intravenous ibuprofen: the first injectable product for the treatment of pain and fever. *J Pain Res*. 2010;3:67–79.
51. Gillespie WR, DiSanto AR, Monovich RE, Albert KS. Relative bioavailability of commercially available ibuprofen oral dosage forms in humans. *J Pharm Sci*. 1982;71(9):1034–8.
52. Evans AM, Nation RL, Sansom LN, Bochner F, Somogyi AA. The relationship between the pharmacokinetics of ibuprofen enantiomers and the dose of racemic ibuprofen in humans. *Biopharm Drug Dispos*. 1990;11(6):507–18.
53. Potthast H, Dressman JB, Junginger HE, Midha KK, Oeser H, Shah VP *et al*. Biowaiver monographs for immediate release solid oral dosage forms: ibuprofen. *J Pharm Sci*. 2005;94(10):2121–2131.33.
54. Henwood SQ, de Villiers MM, Liebenberg W, Lötter AP. Solubility and dissolution properties of generic rifampicin raw materials. *Drug Dev Ind Pharm*. 2000;26(4):403–8.
55. Pähkla R, Lambert J, Ansko P, Winstanley P, Davies PD, Kiivet RA. Comparative bioavailability of three different preparations of rifampicin. *J Clin Pharm Ther*. 1999;24(3):219–25.
56. Chik Z, Basu RC, Pendek R, Lee TC, Mohamed Z. A bioequivalence comparison of two formulations of rifampicin (300- vs 150-mg capsules): An open-label, randomized, two-treatment, two-way crossover study in healthy volunteers. *Clin Ther*. 2010;32(10):1822–31.
57. Rafiq S, Iqbal T, Jamil A, Khan FH. Pharmacokinetic studies of rifampicin in healthy volunteers and tuberculosis patients. *Int J Agric Biol*. 2010;12:391–5.
58. Ruslami R, Nijland MJH, Alisjahbana B, Parwati I, van Crevel R, Rob AE. Pharmacokinetics and tolerability of a higher rifampin dose *versus* the standard dose in pulmonary tuberculosis patients. *Antimicrob Agents Chemother*. 2007;51(7):2546–51.
59. He BX, Shi L, Qiu J, Zeng XH, Tao L, Li R, Hong CJ, Gu XL, Dong FY, Yang L, Zhao SJ. Quantitative determination of atorvastatin and ortho-hydroxy atorvastatin in human plasma by liquid chromatography tandem mass spectrometry and pharmacokinetic evaluation. *Methods Find Exp Clin Pharmacol*. 2010;32(7):481–7.
60. Liu YM, Pu HH, Liu GY, Jia JY, Weng LP, Xu RJ, Li GX, Wang W, Zhang MQ, Lu C, Yu C. Pharmacokinetics and bioequivalence evaluation of two different atorvastatin calcium 10-mg tablets: A single-dose, randomized-sequence, open-label, two-period crossover study in healthy fasted Chinese adult males. *Clin Ther*. 2010;32(7):1396–407.
61. Rao N, Dvorchik B, Sussman N, Wang H, Yamamoto K, Mori A, Uchimura T, Chaikin P. A study of the pharmacokinetic interaction of istradefylline, a novel therapeutic for Parkinson's disease, and atorvastatin. *J Clin Pharmacol*. 2008;48(9):1092–8.
62. Ando H, Tsuruoka S, Yanagihara H, Sugimoto K, Miyata M, Yamazoe Y, Takamura T, Kaneko S, Fujimura A. Effects of grapefruit juice on the pharmacokinetics of pitavastatin and atorvastatin. *Br J Clin Pharmacol*. 2005;60(5):494–7.
63. Arunkumar N, Venkateskumar K, Deecaraman M, Rani C, Mohanraj KP. Preparation and solid state characterization of atorvastatin nanosuspensions for enhanced solubility and dissolution. *Int J PharmTech Research*. 2009;1(4):1725–30.
64. Faasen F, Vromans H. Biowaivers for oral immediate-release products. Implications of linear pharmacokinetics. *Clin Pharmacokinet*. 2004;43(15):1117–26.
65. Szpunar GJ, Albert KS, Bole GG, Dreyfus JN, Lockwood GF, Wagner JG. Pharmacokinetics of flubiprofen in man. I. Area/dose relationships. *Biopharm Drug Dispos*. 1987;8(3):273–83.
66. Nash JF, Bechtol LD, Bunde CA, Bopp RJ, Farid KZ, Spradlin CT. Linear pharmacokinetics of orally administered fenoprofen calcium. *J Pharm Sci*. 1979;68(9):1087–90.
67. McAllister WA, Winfield CR, Collins JV. Pharmacokinetics of prednisolone in normal and asthmatic subjects in relation to dose. *Eur J Clin Pharmacol*. 1981;20(2):141–5.
68. Bauer-Brandl A. Polymorphic transitions of cimetidine during manufacture of solid dosage forms. *Int J Pharmaceutics*. 1996;140(2):195–206.
69. Grahnen A, Bahr C, Lindström B, Rosén A. Bioavailability and pharmacokinetics of cimetidine. *Eur J Clin Pharmacol*. 1979;16(5):335–40.